Medical Dosimetry 42 (2017) 97–103

Medical Dosimetry

journal homepage: www.meddos.org

Dosimetry Contribution:

Functional image-guided stereotactic body radiation therapy planning for patients with hepatocellular carcinoma

Uranchimeg Tsegmed, M.D.,* Tomoki Kimura, M.D., Ph.D.,* Takeo Nakashima, Ph.D.,† Yuko Nakamura, M.D., Ph.D.,‡ Toru Higaki, Ph.D.,‡ Nobuki Imano, M.D.,* Yoshiko Doi, M.D.,* Masahiro Kenjo, M.D., Ph.D.,* Shuichi Ozawa, Ph.D.,* Yuji Murakami, M.D., Ph.D.,* Kazuo Awai, M.D., Ph.D.,‡ and Yasushi Nagata, M.D., Ph.D.*

*Department of Radiation Oncology, Graduate School of Biomedical and Health Sciences, Hiroshima University, Hiroshima, Japan; †Division of Radiation Therapy, Hiroshima University Hospital, Hiroshima, Japan; and ‡Department of Diagnostic Radiology, Graduate School of Biomedical and Health Sciences, Hiroshima University, Hiroshima, Japan

ARTICLE INFO

Article history:
Received 16 May 2016
Received in revised form 12 January 2017
Accepted 28 January 2017

Keywords:
Functional image-guided radiotherapy
SBRT
Hepatocellular carcinoma
Gadoxetate disodium-enhanced MRI

ABSTRACT

The aim of the current planning study is to evaluate the ability of gadoxetate disodium-enhanced magnetic resonance imaging (EOB-MRI)–guided stereotactic body radiation therapy (SBRT) planning by using intensity-modulated radiation therapy (IMRT) techniques in sparing the functional liver tissues during SBRT for hepatocellular carcinoma. In this study, 20 patients with hepatocellular carcinoma were enrolled. Functional liver tissues were defined according to quantitative liver-spleen contrast ratios ≥ 1.5 on a hepatobiliary phase scan. Functional images were fused with the planning computed tomography (CT) images; the following 2 SBRT plans were designed using a "step-and-shoot" static IMRT technique for each patient: (1) an anatomical SBRT plan optimization based on the total liver; and (2) a functional SBRT plan based on the functional liver. The total prescribed dose was 48 gray (Gy) in 4 fractions. Dosimetric parameters, including dose to 95% of the planning target volume (PTV $D_{95\%}$), percentages of total and functional liver volumes, which received doses from 5 to 30 Gy (V5 to V30 and fV5 to fV30), and mean doses to total and functional liver (MLD and fMLD, respectively) of the 2 plans were compared. Compared with anatomical plans, functional image-guided SBRT plans reduced MLD (mean: plan A, 5.5 Gy; and plan F, 5.1 Gy; $p < 0.0001$) and fMLD (mean: plan A, 5.4 Gy; and plan F, 4.9 Gy; $p < 0.0001$), as well as V5 to V30 and fV5 to fV30. No differences were noted in PTV coverage and nonhepatic organs at risk (OARs) doses. In conclusion, EOB-MRI–guided SBRT planning using the IMRT technique may preserve functional liver tissues in patients with hepatocellular carcinoma (HCC).

Introduction

Hepatocellular carcinoma (HCC) is the sixth most common cancer and the third leading cause of cancer-related death in the world.[1] Curative therapy for early-stage HCC involves surgeries such as resection or transplantation.[2,3] However, only 10% to 30% of patients with HCC are eligible for surgery.[4] Accordingly, for patients with HCC with liver dysfunction, underlying cirrhosis, or multifocal tumors, locoregional therapies such as radiofrequency ablation or transarterial chemoembolization are recommended.[3] Although radiation therapy has not been accepted as a therapeutic option for HCC according to the Barcelona Clinic Liver Cancer staging system, several studies have reported good treatment outcomes with stereotactic body radiation therapy (SBRT) for HCC.[5-7] SBRT is a highly conformal radiotherapy (RT) technique used for extracranial tumors, which delivers a very high dose per fraction in a short time while limiting the exposure to adjacent normal tissues.[8,9]

Challenges of HCC treatment include limited liver function in some patients; in previous studies, nonclassic radiation-induced liver disease (RILD) was more common in patients with poor liver function (hepatitis B infection and Child-Pugh classes B and C).[10,11] Therefore, SBRT to the liver should be cautiously planned to prevent RILD. Moreover, the incidence of RILD is strongly correlated with irradiated liver volumes[12] and mean liver doses.[13] Hence, precise assessments of liver function are critical to minimize irradiated volumes and mean doses to functional liver tissues.

Functional imaging techniques are used during RT planning and treatment to minimize irradiated volumes and mean doses to functional tissues while delivering highly conformal doses to the tumor.[14]

Reprint requests to Tomoki Kimura, M.D., Ph.D., Department of Radiation Oncology, Graduate School of Biomedical and Health Sciences, Hiroshima University, 1-2-3 Kasumi, Minami-ku, Hiroshima City, 734-8551, Japan.
E-mail: tkkimura@hiroshima-u.ac.jp

http://dx.doi.org/10.1016/j.meddos.2017.01.005
0958-3947/Copyright © 2017 American Association of Medical Dosimetrists

Functional imaging modalities, such as functional magnetic resonance imaging (MRI),[15] [^{18}F]-fluorodeoxyglucose positron emission tomography,[16] single-photon emission computed tomography (SPECT) using 99mTc-labeled iminodiacetic acid,[17] and 4-dimensional computed tomography (CT),[18] have been used during radiation treatment planning. However, functional image-guided RT planning and treatment for HCC remain poorly validated. A few studies investigated the efficacy of SPECT-based RT for HCC[19,20]; however, in clinical practice, SPECT liver imaging for liver SBRT is implemented in several institutions only.

Recent studies indicate that gadoxetate disodium (EOB; EOB Primovist; Bayer Yakuhin Ltd., Osaka, Japan)-enhanced MRI (EOB-MRI) is effective for detecting hepatic lesions and may indicate hepatic function.[21,22] Some studies have demonstrated the clinical utility of EOB-MRI as a predictive parameter to assess the changes in hepatic function after SBRT.[23,24] Thus, it is a promising imaging technique for assessing liver dysfunction and predicting changes in hepatic function after SBRT. Therefore, we believe that the EOB-MRI–guided liver functional imaging modality can be applied to SBRT for liver cancer to spare the functional liver region using intensity-modulated radiation therapy (IMRT) planning and lead to safer and more efficacious treatment.

Here we investigated the ability of EOB-MRI–guided SBRT planning using IMRT techniques to reduce functional liver mean dose and functional liver volumes, which received doses from 5 to 30 Gy.

Methods and Materials

Patient characteristics

A total of 20 subjects were recruited after curative SBRT for HCC at Hiroshima University Hospital between May 2009 and May 2013. The study was approved by the university's Human Ethics Review Committee, and written informed consent was obtained from all patients.

The inclusion criteria of our institution for curative SBRT for HCC are as follows: (1) Eastern Cooperative Oncology Group Performance Status of 0 to 2; (2) Child-Pugh score A or B; (3) < 3 HCC nodules, each less than 5 cm in diameter, with or without vascular invasion; (4) luminal gastrointestinal tract should be far from tumor more than 2 cm; (5) inoperability; and (6) unsuitability for radiofrequency ablation because of tumor location, invisibility on ultrasonography, or bleeding tendency. The exclusion criteria were uncontrolled ascites and gastrointestinal tract-adjacent tumor.

Patient and tumor characteristics are summarized in Table 1.

EOB-MRI acquisition

MRI was performed before SBRT planning for all patients using 1.5-T imagers (Signa Excite HD; GE Healthcare, Milwaukee, WI) and an 8-channel body-phased array coil. Respiratory motion was controlled using the breath-hold method at the end of the expiratory phase. Dynamic MRI was performed with fat-suppressed T1-weighted gradient-echo imaging and 3-dimensional (3D) acquisition sequences (liver acquisition with volume acceleration). After pre-enhanced scanning, EOB was administered intravenously and 4-phase EOB-enhanced scans of the liver were obtained during the arterial, portal venous, transitional,[25] and hepatobiliary phase (HBP). Scanning during the HBP was performed from 20 minutes after the start of EOB injections.

Table 1
Patient and tumor characteristics

Age	Median/(range)	73/(55-84)
Sex	Male/Female	12/8
Performance status	0/1	18/2
Type of virus infection	HCV/HBV/NBNC	18/1/1
Child-Pugh class	A/B	17/3
Child-Pugh score	5/6/7/≥ 8	10/7/3/0
Clinical stage [UICC Seventh]	I/II	14/6
TMN	T1N0M0/T2N0M0	14/6
Tumor location	S3/S4/S5/S6/S7/S8	2/3/1/4/4/6
GTV (cm^3)	Median/(range)	1.7/(0.03-27.6)
PTV (cm^3)	Median/(range)	16.2/(2.4-87.3)

GTV, gross tumor volume; HBV, hepatitis B virus; HCV, hepatitis C virus; NBNC, nonhepatitis B nonhepatitis C; PTV, planning target volume; S, segment of liver; UICC, International Union Against Cancer.

EOB (25 μmol/kg) was administered at a rate of 2.0 mL/s and then flushed using 20 mL of saline with a power injector (Sonic Shot 50; Nemoto Kyorindo, Tokyo, Japan). All of the images were obtained in the transverse plane with an acquisition time of 20 seconds, and 3-mm-thick HBP images were used to generate a functional liver map.

CT acquisition for SBRT planning

Patients were immobilized with a vacuum cushion (Vac-Lok with Wingboard; CIVCO, Orange City, Iowa), and respiratory motion was coordinated by voluntary breath-holding in the end of the expiratory phase using an Abches device (Apex Medical, Tokyo, Japan) that allows patients to control the respiratory motion of the chest and abdomen. For the simulations, dynamic CT scans (LightSpeed QX/I; GE Medical Systems, Waukesha, WI) included noncontrast enhancement, and images in the arterial, portal, and venous phases were collected following the bolus injections of nonionic iodinated contrast material (100 mL at 3 mL/s). CT slice thicknesses were 1.25 to 2.5 mm.

Functional liver map construction

Functional liver maps were generated using a 4-step procedure based on the EOB-MRI and SBRT planning CT images (Fig. 1). Both image types were acquired before the radiation planning, and assessments of liver function were performed using the EOB-MRI and planning CT images as a spatial reference. At first deformable registration, EOB-MRI was spatially aligned using planning CT with an insight segmentation and registration toolkit.[26] For median filtering, the EOB-MRI images were smoothed using a 3D median filter ($15 \times 15 \times 15$ mm). For liver-spleen contrast ratio (LSC) conversion, the MRI signals were then converted to a functional map according to quantitative LSC. The pixels of the EOB-MRI images were divided according to spleen signal intensities, which were measured manually using the volumetric region of interest. Functional liver was defined as quantitative LSC ≥ 1.5 during the HBP as described previously.[27] Functional liver maps were posterized from gradation images to stepped images by rounding of the numbers to the nearest decimal point for ease of analysis (> 1.0 but < 1.1, rounded to 1.0; > 1.1 but < 1.2, rounded to 1.1). Finally, because a treatment planning system does not accommodate decimal numbers on images, the functional map values were multiplied by 1000.

SBRT planning

RT planning CT and EOB-MRI images from 20 patients were transferred to a 3D treatment planning system (Pinnacle3 ver. 9.6; Phillips Medical Systems, Fitchburg, WI). The EOB-MRI images were then fused with the planning CT images that were obtained during the arterial phase.

Gross tumor volumes (GTVs) were defined as those carrying residual lipiodol using transarterial chemoembolization and early enhancement during the arterial phase of dynamic CT. A clinical target volume (CTV) margin of 0 to 5 mm was added to the GTV for subclinical invasions, and a planning target volume (PTV) margin of 5 to 8 mm was added to the CTV based on the reproducibility of respiratory motions and setup errors. Eight ports were selected in all patients, including 4 coplanar and 4 noncoplanar static beams, which were established in directions that avoided the stomach, intestine, gall bladder, and spine, if possible. Treatment plans were delivered using 6- and 10-MV photons generated by a linear accelerator (Clinac iX; Varian Medical Systems, Palo Alto, CA). The total prescribed dose was 48 gray (Gy) in 4 fractions and the prescription dose was delivered to 95% of the PTV.

SBRT plans were subsequently designed using a "step-and-shoot" static IMRT technique for each patient. First of all, the anatomical SBRT plan (plan A) was optimized based on total liver volume using the clinical optimization parameters. Plan A's optimization parameters were copied in the functional SBRT plan (plan F), and then the functional liver map (volume) was added to the dose constraints of plan F. Finally, plan F was re-optimized based on the functional liver volume. Table 2 shows the dose constraints for plans A and F, which had exactly the same IMRT optimized values for each patient but different functional liver values.

IMRT inverse treatment planning was optimized using a direct machine parameter optimization algorithm. Dose calculations were performed using a $2 \times 2 \times 2$ mm dose grid and a dose computation with collapsed cone convolution.

Data analysis and statistical methods

Dosimetric parameters of plans A and F were investigated by (1) PTV doses to 95% of the prescription dose (PTV $D_{95\%}$) and mean PTV dose; (2) calculating mean doses to total and functional liver minus GTVs (MLD and fMLD), respectively; (3) expressing percentages of total and functional liver volumes, which received doses from 5 to 30 Gy (V5 to V30, fV5 to fV30); (4) calculating mean doses, doses to 0.5 cc and to 5 cc volumes (D0.5cc and D5cc) of the stomach, duodenum, and intestine; and (5) calculating monitor units.

Statistical analyses were performed using R-statistics program version 3.1.2 (The R Foundation for Statistical Computing, Vienna, Austria). Differences were identified using paired t-tests and considered significant at values of $p < 0.05$. All quantitative data are expressed as mean ± standard deviation.

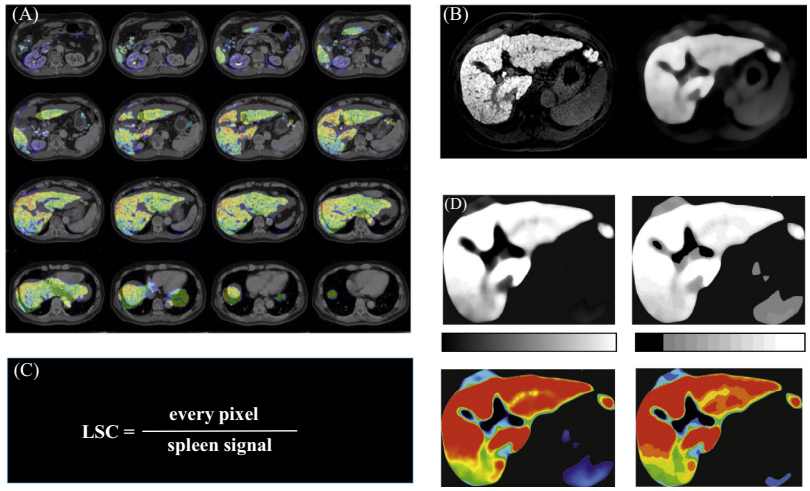

Fig. 1. Protocol for generating functional liver maps based on planning CT and gadoxetate disodium-enhanced magnetic resonance imaging (EOB-MRI). (A) Deformable registration: basal image (grayscale), planning CT; overlaid color image, EOB-MRI. (B) Median filtering: (left) prefiltering EOB-MRI; (right) postfiltering EOB-MRI. (C) Liver-spleen contrast ratio conversion; EOB-MRI pixels divided by the spleen's signal intensity. (D) Posterization: EOB-MRI before (upper left) and after (upper right) posterization; colored EOB-MRI before (lower left) and after (lower right) posterization.

Table 2
Dose constraints for anatomical and functional intensity modulated radiotherapy plans

ROI	Plan A: Anatomical plan				Plan F: Functional plan			
	Constraint	Dose (cGy)	Volume (%)	Weight	Constraint	Dose (cGy)	Volume (%)	Weight
GTV								
Max DVH		6100	0	1		6100	0	1
Min DVH	✓	6000	1		✓	6000	1	
Min DVH		5000	90	1		5000	90	1
PTV								
Max DVH		6100	0	80		6100	0	80
Max DVH		4848	95	100		4848	95	100
Min DVH	✓	4800	95		✓	4800	95	
Min Dose		4320	—	100		4320	—	100
PTV + 20 mm_ring								
Max DVH		2000	0	80		2000	0	80
PTV + 5 mm_ring								
Max DVH		4300	0	50		4300	0	50
Max DVH		2000	50	10		2000	50	10
Spinal cord								
Max DVH		1200	0	10		1200	0	10
Stomach								
Max DVH		1800	0	10		1800	0	10
Liver–GTV								
Max DVH		2000	5	1-5		2000	5	1-5
Liver_avoid								
Max DVH		1800	5	5		1800	5	5
Functional liver–GTV								
Max DVH						1800	5	1-5
Functional liver_avoid								
Max DVH						1500	5	5

GTV, gross tumor volume; Liver_avoid, add ring-shaped 10-mm-thick ROI to PTV and then the ROI is avoided interior to total liver; Max DVH, maximum dose-volume histogram; Min DVH, minimum dose-volume histogram; PTV, planning target volume; PTV + 20 mm_ring, ring-shaped ROI margin of 20 mm is added to PTV; ROIs, regions of interest.

Results

Comparison of dosimetric parameters for PTV

Dosimetric parameters including PTV $D_{95\%}$ (mean: plan A, 48.0; plan F, 48.0 Gy; $p = 0.78$) and mean PTV doses (mean: plan A, 54.6 Gy; and plan F, 54.8 Gy; $p = 0.11$) did not differ significantly between the 2 plans.

Comparison of dosimetric parameters for total and functional livers

Compared with plan A, plan F significantly reduced MLD (mean: plan A, 5.5 Gy; plan F, 5.1 Gy; $p < 0.0001$) and fMLD (mean: plan A, 5.4 Gy; plan F, 4.9 Gy; $p < 0.0001$) as well as total and functional liver V5 to V30 and fV5 to fV30 while maintaining the target dose coverage.

Moreover, plan F, which was optimized additionally with functional liver volume, reduced the numbers of low-dose areas (Figs. 2

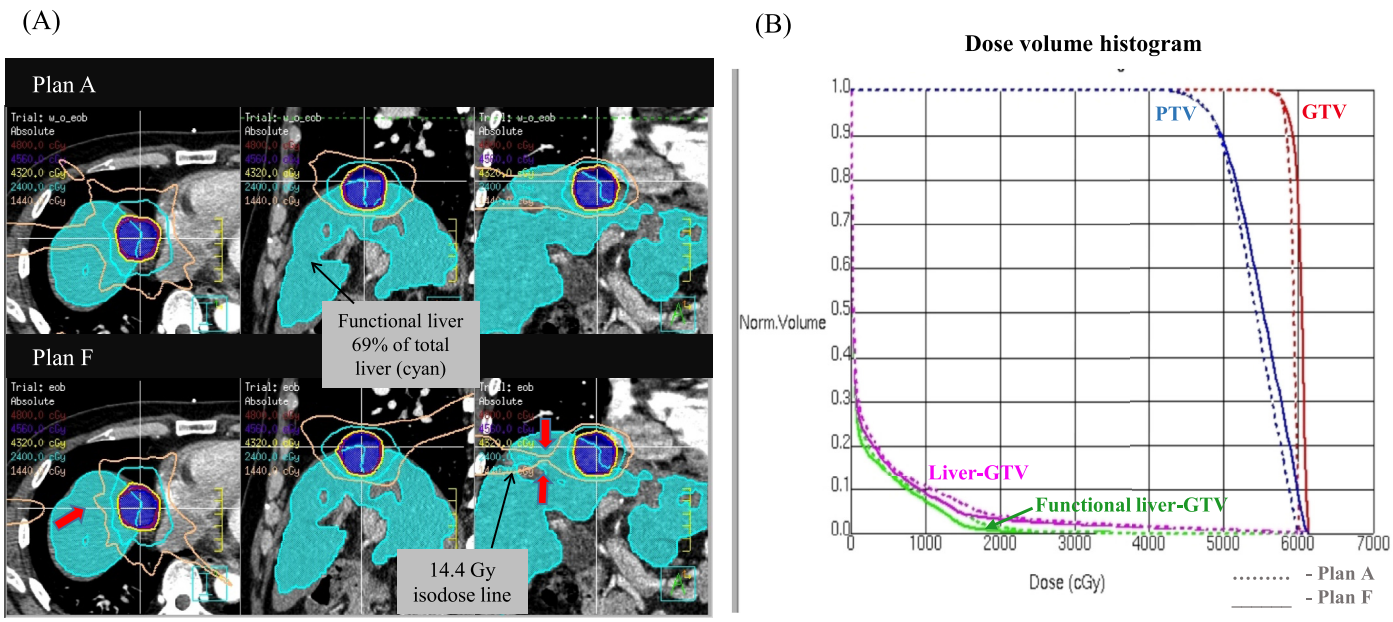

Fig. 2. Comparisons of the dose distribution maps and dose-volume histograms between anatomical stereotactic body radiation therapy (SBRT) (plan A) and functional SBRT plans (plan F) in a patient (patient E) with a large functional liver volume; 69% of total liver: cyan. (A) Dose distribution maps of axial, sagittal, and coronal sections of plan A (upper) and plan F (lower) are presented. The isodose line at 14.4 Gy (almond) is significantly reduced (red arrows) in the functional plan. (B) Dose-volume histograms of plan A (dash line) and plan F (solid line) for patient E. Planning target volume (PTV) and gross tumor volume (GTV) did not differ significantly between the 2 plans; however, mean doses to total and functional liver minus GTV of the 2 plans were significantly reduced in plan F.

and 3; arrows) and spared the functional hepatic parenchyma. Dose-volume histograms of patients with small functional liver volumes (Fig. 3B) show marked reductions in mean liver doses, particularly in fMLD, compared with patients with large functional liver volumes (Fig. 2B).

Comparison of dosimetric parameters for gastrointestinal organs

Mean dose, D0.5cc, and D5cc of the stomach (mean: plan A, 0.82 Gy; plan F, 0.78 Gy; $p = 0.19$; D0.5cc: plan A, 6.0 Gy; plan F, 5.8 Gy; $p = 0.34$; D5cc: plan A, 4.5 Gy; plan F, 4.4 Gy; $p = 0.36$), duodenum (mean: plan A, 0.59 Gy; plan F, 0.62 Gy; $p = 0.09$; D0.5cc: plan A, 2.2 Gy; plan F, 2.4 Gy; $p = 0.07$; D5cc: plan A, 0.96 Gy; plan F, 0.98 Gy; $p = 0.4$), and intestine (mean: plan A, 0.68 Gy; plan F, 0.66 Gy; $p = 0.29$; D0.5cc: plan A, 4.5 Gy; plan F, 4.7 Gy; $p = 0.36$; D5cc: plan A, 3.1 Gy; plan F, 3.1 Gy; $p = 0.45$) were not significantly different in the two plans. However, monitor units (mean: plan A, 2437; plan F, 2495; $p = 0.01$) and conformity indexes (mean: plan A, 0.99; plan F, 1.01; $p = 0.003$) differed significantly between the 2 plans. Comparison of the dosimetric parameters between plan A and plan F is summarized in Table 3.

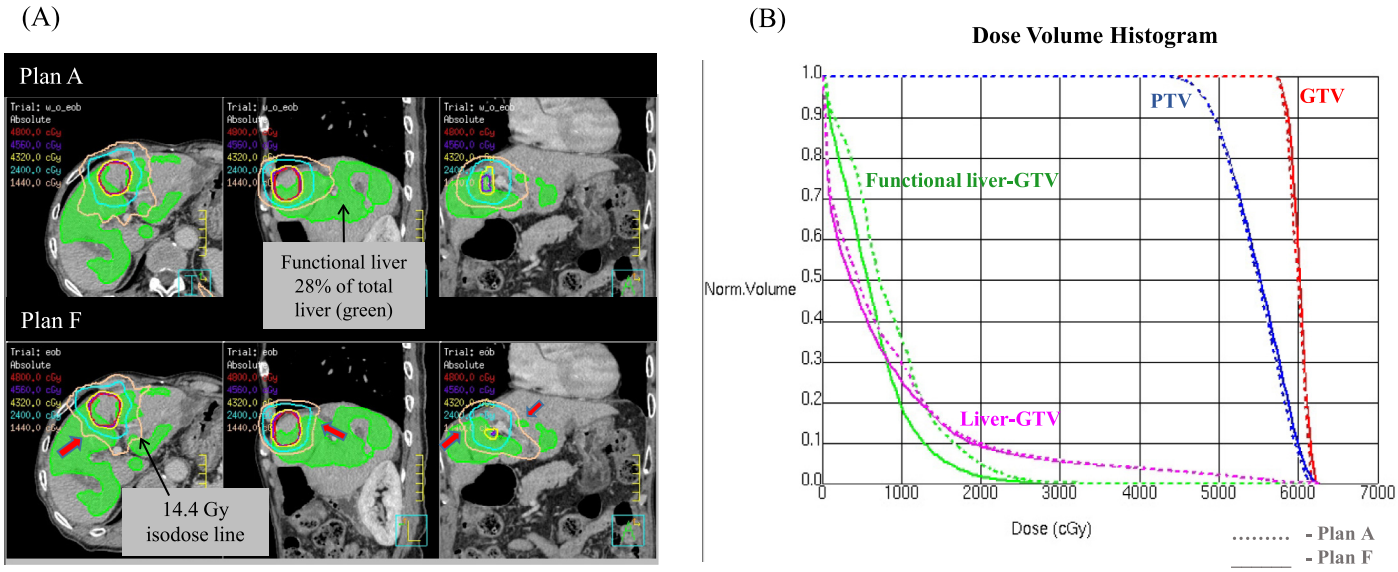

Fig. 3. Comparison of dose distribution maps and dose-volume histograms between anatomical SBRT (plan A) and functional SBRT plans (plan F) in patient A with a small functional liver volume; 28% of total liver: green. (A) Dose distribution maps of axial, sagittal, and coronal sections of plan A (upper) and plan F (lower) are shown. Isodose lines at 14.4 (almond) and 24 Gy (cyan) are clearly reduced (red arrows) in the functional plan. (B) Dose-volume histogram of plan A (dash line) and plan F (solid line) for patient A. Planning target volume (PTV) and gross tumor volume (GTV) did not differ between the 2 plans; however, mean doses to total and functional liver minus GTV were clearly decreased in plan F.

Table 3
Comparison of dosimetric parameters between anatomical and functional plans

ROI	Plan A	Plan F	*p*-value
PTV:			
D95 (Gy)	48.0 ± 0.02	48.0 ± 0.015	0.78
Mean dose (Gy)	54.6 ± 0.55	54.8 ± 0.62	0.11
Conformity index	0.99 ± 0.06	1.01 ± 0.07	0.003
Total liver GTV:			
Mean dose (Gy)	5.5 ± 2.7	5.1 ± 2.7	<0.0001
V5 (%)	30 ± 14	27 ± 14.6	0.0002
V10 (%)	18 ± 11	16 ± 11	<0.0001
V15 (%)	11 ± 7.6	9.4 ± 6.4	0.0004
V20 (%)	6.6 ± 4.4	6.3 ± 4	0.006
V25 (%)	4.6 ± 2.9	4.5 ± 2.9	0.01
V30 (%)	3.53 ± 2.2	3.46 ± 2.2	0.03
Functional liver GTV:			
Mean dose (Gy)	5.4 ± 2.9	4.9 ± 2.7	<0.0001
fV5 (%)	31 ± 18	28 ± 17	0.002
fV10 (%)	18 ± 12	15 ± 10	0.0006
fV15 (%)	10.6 ± 7.6	8.7 ± 5.5	0.001
fV20 (%)	6.4 ± 4.2	5.7 ± 3.6	0.01
fV25 (%)	4.4 ± 2.8	4.2 ± 2.6	0.01
fV30 (%)	3.3 ± 2	3.1 ± 1.9	0.01
Stomach			
Mean dose (Gy)	0.82 ± 0.76	0.78 ± 0.78	0.19
D0.5cc (Gy)	6.0 ± 5.0	5.8 ± 5.5	0.34
D5cc (Gy)	4.5 ± 4.5	4.4 ± 4.9	0.36
Duodenum			
Mean dose (Gy)	0.59 ± 0.96	0.62 ± 1	0.09
D0.5cc (Gy)	2.2 ± 3.7	2.4 ± 4	0.07
D5cc (Gy)	0.96 ± 2.4	0.98 ± 2.5	0.4
Intestine*			
Mean dose (Gy)	0.68 ± 1.1	0.66 ± 1	0.29
D0.5cc (Gy)	4.5 ± 5.7	4.7 ± 6.4	0.36
D5cc (Gy)	3.1 ± 4.4	3.1 ± 4.8	0.45
Monitor unit	2437 ± 366	2495 ± 378	0.01

D0.5cc, dose to 0.5 cc volumes; D5cc, dose to 5 cc volumes; D95, dose to 95% of PTV; fV5 to fV30, percentage of functional liver volumes, which received doses from 5 to 30 Gy; GTV, gross tumor volume; Plan A, anatomical plan; Plan F, functional plan; PTV, planning target volume; ROI, region of interest; V5 to V30, percentage of total liver volumes, which received doses from 5 to 30 Gy.
* Intestine includes small and large bowels.

Discussion

The present simulation study shows the ability of functional EOB-MRI–guided liver SBRT planning with IMRT technique to spare functional liver.

SPECT scintigraphic methods are currently the only imaging-based liver function tests that are used in clinical practice and are predominantly performed using 99mTc-iminodiacetate analogs. Although SPECT with 99mTc-mebrofenin or 99mTc-galactosyl human serum albumin indicates hepatic function, it is difficult to use in conjunction with SBRT, reflecting limitations such as low temporal and spatial image resolution,[28] inability to control internal organ motion during long scan periods, additional radiation dose exposure, and cost. In contrast, EOB-MRI has the potential to quantify liver perfusion and function, and is commonly used in many institutions. Approximately 50% of the EOB is taken up by hepatocytes after injection into normal human livers,[29,30] allowing the distinction of functional (EOB-loaded) and dysfunctional liver parenchyma.[31,32] The enhancement of the liver at EOB-MRI depends on liver perfusion, vascular permeability, extracellular diffusion, and hepatocyte transporter expression.[33] Additionally, Verloh *et al.* demonstrated the utility of EOB-MRI and relative EOB-MRI enhancement during the HBP as image-based tests of regional and global liver function.[22]

Among the advantages of EOB-MRI guidance for liver SBRT is that EOB-MRI immediately distinguishes between functional and dysfunctional liver tissues with accuracy similar to that of SPECT. Geisel *et al.* suggested that EOB-MRI and 99mTc-mebrofenin hepatobiliary scintigraphy can be used to separately determine right and left liver lobe function.[34]

EOB-MRI can also be applied to SBRT planning for HCC. Because the liver can move substantially because of breathing, breath-holding or immobilization techniques must be used to obtain high-quality image registration between functional image sets and treatment planning sets. In particular, MRI scanning takes approximately 20 seconds, enabling control of the liver motion during the end-expiratory phase as performed for planning CT. Other advantages of EOB-MRI include the absence of radiation and relative cost-effectiveness compared with positron emission tomography or SPECT. Furthermore, EOB-MRI can be used routinely in clinical practice because most hospitals have MRI instruments.

Different EOB-MR imaging parameters, such as LSC, corrected liver-enhancement ratio, and contrast enhancement indexes, have been used as imaging-based liver function and fibrosis markers.[35,36] However, which of the various existing imaging markers would provide the most accurate information on liver function is a matter of much controversy and debate. In this study, functional liver maps were generated according to quantitative LSC ≥ 1.5 in the HBP as described by Motosugi *et al.*[27,37] According to their studies, the quantitative LSC during HBP appears to have a statistically significant correlation with indocyanine green clearance test and Child-Pugh classification. Moreover, patients with quantitative LSC of more than 1.5 have been evaluated with good or excellent score of visual LSC.[37]

This study indicated that EOB-MRI–guided functional imaging modality can be applied to liver SBRT to distinguish functional liver regions. Moreover, in a prospective study by Shirai *et al.*, 3D conformal radiotherapy using SPECT with 99mTc-galactosyl human serum albumin was shown to be well tolerated by patients with unresectable HCC and portal vein tumor thrombi, and no patients experienced RILD.[20] Hence, EOB-MRI–guided SBRT plan for the liver could be a clinically applicable technique and be used to minimize doses to normal liver tissues. Further prospective clinical trial is needed to demonstrate the clinical impact of the functional SBRT plan.

In this study, the dose constraints of PTV, normal liver, and nonhepatic organs at risk (OARs) complied with protocol of the Radiation Therapy Oncology Group 1112 clinical trial of SBRT for HCC and recommendation of the Quantitative Analyses of Normal Tissue Effects in the Clinic to reduce the risk of hepatic and gastrointestinal toxicity. The Quantitative Analysis of Normal Tissue Effects in Clinic recommendations for liver SBRT are as follows: MLD (liver minus GTV) should receive < 13 Gy for HCC, in 3 fractions; < 18 Gy for HCC, in 6 fractions; < 6 Gy for HCC, Child-Pugh B, in 4 to 6 Gy per fraction, or that MLD of ≥ 700 mL of normal liver should receive ≤ 15 Gy in 3 to 5 fractions.[11]

The protocol of Radiation Therapy Oncology Group 1112 liver trial recommends “reducing the maximal dose to all luminal gastrointestinal normal tissues should be a planning priority to minimize the risk of gastrointestinal toxicity.” The following gastrointestinal organ dose constraints were recommended by the protocol: maximum dose for stomach, duodenum, and intestine should receive < 30 Gy to 0.5 cc and < 25 Gy to 5 cc separately.[38]

The present results showed that total and functional liver mean doses (MLD, fMLD) and nonhepatic OARs doses were much lower than their dose constraints. Stomach, duodenum, and intestine doses, which are OARs of interest with liver SBRT, were not significantly different in the 2 plans (Table 3).

Furthermore, this study demonstrated that an excellent dose distribution and preserving functional liver can be made by functional EOB-MRI–guided SBRT planning using IMRT technique. It was able to make an excellent dose distribution and to reduce dose to the functional liver, as well as the total liver by optimizing additional dose constraints for the functional liver with IMRT inverse planning technique. The current results showed that the degree of

functional preservation depends on functional liver tissue location and volume, as well as tumor location and size. Specifically, functional image-guided SBRT planning was more efficient in patients with small functional liver volumes (Fig. 3) than in those with large functional liver volumes (Fig. 2). Previous studies also demonstrated the dependence of dosimetric benefits on functional region location and volumes,[14,39] with greater dosimetric preservation of functional lung tissues in patients with heterogeneous functional distributions that do not completely surround the target. Moreover, Lavrenkov *et al.* showed that IMRT led to greater preservation of the functional lung volume when the functional lung was located proximal to the PTV and when the overall functional distribution was more heterogeneous.[39]

Accurate image registration and delineation of targets and normal tissues are critical to the utility of functional image guidance during RT planning. Thus, we generated a functional liver map with high spatial resolution and image resolution using the methods presented above and demonstrated the ease of fusing EOB-MRI images to planning CT images and delineating the functional liver map.

The main limitation of the current study is that it is only a simulation study on a small cohort, warranting further prospective clinical trials of large patient populations. Second, the registration of EOB-MRI and RT planning CT images was compromised by imperfect image matching in some cases, for which the deformable imaging software required manual adjustments to achieve high focus on the target, vessel, and peripheral shape areas. Finally, the functional liver regions were determined using a binary quantitative criterion (LSC ≥ 1.5). Thus, the inclusion of additional imaging markers in further analyses would be beneficial to define quantitatively the functional heterogeneity.

Conclusions

This simulation study demonstrates the ability of functional imaging with EOB-MRI for SBRT planning in patients with HCC. EOB-MRI–guided SBRT planning using the IMRT technique may improve functional liver preservation in patients with HCC.

Conflict of Interest

None of the contributing authors declares an ethical or financial conflict of interest.

Authors' Contributions

U.T. contributed to the study design, literature search, data acquisition, data analysis, data interpretation, statistical analysis, manuscript preparation, and manuscript editing. T.K. contributed to study conception and design, data acquisition, data analysis, data interpretation, statistical analysis, manuscript editing, and manuscript review. T.N. contributed to the data acquisition, data analysis, data interpretation, statistical analysis, manuscript editing, and manuscript review. T.H., Y. Nakamura, and K.A. made substantial contributions to the EOB-MRI acquisition, functional liver map creation, data interpretation, and manuscript editing and reviewing. N.I. and Y.D. participated in the data acquisition, data analysis, and data interpretation. M.K., S.O., Y.M., and Y. Nagata made substantial intellectual contributions to the article revision, data acquisition, data analysis, and data interpretation processes. All authors approved the final version for publication.

Acknowledgments

This work was supported in part by the Hiroshima University Phoenix Leader Education Program for the "Renaissance from Radiation Disaster" funded by the Ministry of Education, Culture, Sports, Science and Technology of Japan. The authors thank Dr. May Abdel-Wahab for her professional advice.

References

1. Ferlay, J.; Soerjomataram, I.; Ervik, M.; *et al*, *GLOBOCAN 2012 v1.0, Cancer Incidence and Mortality Worldwide: IARC Cancer Base No. 11*. Lyon, France: International Agency for Research on Cancer; 2013. Available at: http://globocan.iarc.fr. Accessed April 12, 2015.
2. Thomas, M.B.; Jaffe, D.; Choti, M.M.; *et al*. Hepatocellular carcinoma: consensus recommendations of the national cancer institute clinical trials planning meeting. *J. Clin. Oncol.* **28**(25):3994–4005; 2010.
3. European Association for the Study of the Liver; European Organisation for Research and Treatment of Cancer. EASL-EORTC clinical practice guidelines: management of hepatocellular carcinoma. *J. Hepatol.* **56**(4):908–43; 2012.
4. Choi, E.; Rogers, E.; Ahmad, S.; *et al*. Hepatobiliary cancers. In: Feig, B.W.; Berger, D.H.; Fuhrman, G.M.; eds. *The M.D. Anderson Surgical Oncology Handbook*. Philadelphia, PA: Lippincott Williams & Wilkins. 320–66; 2006.
5. Kimura, T.; Aikata, H.; Takahashi, S.; *et al*. Stereotactic body radiotherapy for patients with small hepatocellular carcinoma ineligible for resection or ablation therapies. *Hepatol. Res.* **45**(4):378–86; 2015.
6. Bibault, J.E.; Dewas, S.; Vautravers-Dewas, C.; *et al*. Stereotactic body radiation therapy for hepatocellular carcinoma: prognostic factors of local control, overall survival, and toxicity. *PLoS ONE* **8**(10):e77472; 2013.
7. Jang, W.I.; Kim, M.S.; Bae, S.H. High-dose SBRT correlates increased local control and overall survival in patients with inoperable hepatocellular carcinoma. *Radiat. Oncol.* **8**(250):1–12; 2013.
8. Yoon, S.M.; Lim, Y.S.; Park, M.J.; *et al*. Stereotactic body radiation therapy as an alternative treatment for small hepatocellular carcinoma. *PLoS ONE* **8**(11):2013. e79854.
9. Lee, I.J.; Seong, J. The optimal selection of radiotherapy treatment for hepatocellular carcinoma. *Gut Liver* **6**(2):139–48; 2012.
10. Liang, S.X.; Zhu, X.D.; Xu, Z.Y.; *et al*. Radiation-induced liver disease in three-dimensional conformal radiation therapy for primary liver carcinoma: the risk factors and hepatic radiation tolerance. *Int. J. Radiat. Oncol. Biol. Phys.* **65**(2):426–34; 2006.
11. Pan, C.C.; Kavanagh, B.D.; Dawson, L.A.; *et al*. Radiation-associated liver injury. *Int. J. Radiat. Oncol. Biol. Phys.* **76**(3):S94–100; 2010.
12. Lee, I.J.; Seong, J.; Shim, S.J.; *et al*. Reappraisal of risk factors predicting liver complications from radiotherapy for hepatocellular carcinoma. *Korean J. Hepatol.* **12**(3):420–8; 2006.
13. Dawson, L.A.; Normolle, D.; Balter, J.M.; *et al*. Analysis of radiation-induced liver disease using the Lyman NTCP model. *Int. J. Radiat. Oncol. Biol. Phys.* **53**(4):810–21; 2002.
14. Das, S.K.; Ten Haken, R.K. Functional and molecular image guidance in radiotherapy treatment planning optimization. *Semin. Radiat. Oncol.* **21**(2):111–8; 2011.
15. Cao, Y. The promise of dynamic contrast-enhanced imaging in radiation therapy. *Semin. Radiat. Oncol.* **21**(2):147–56; 2011.
16. Eo, J.S.; Paeng, J.C.; Lee, D.S. Nuclear imaging for functional evaluation and theragnosis in liver malignancy and transplantation. *World J. Gastroenterol.* **20**(18):5375–88; 2014.
17. Wang, H.; Feng, M.; Frey, K.A.; *et al*. Predictive models for regional hepatic function based on 99mTc-IDA SPECT and local radiation dose for physiologic adaptive radiation therapy. *Int. J. Radiat. Oncol. Biol. Phys.* **86**(5):1000–6; 2013.
18. Kimura, T.; Nishibuchi, I.; Murakami, Y.; *et al*. Functional image-guided radiotherapy planning in respiratory-gated intensity-modulated radiotherapy for lung cancer patients with chronic obstructive pulmonary disease. *Int. J. Radiat. Oncol. Biol. Phys.* **82**(4):e663–70; 2012.
19. Shen, S.; Jacob, R.; Bender, L.W.; *et al*. A technique using 99mTc-mebrofenin SPECT for radiotherapy treatment planning for liver cancers or metastases. *Med. Dosim.* **39**(1):7–11; 2014.
20. Shirai, S.; Sato, M.; Suwa, K.; *et al*. Single photon emission computed tomography-based three-dimensional conformal radiotherapy for hepatocellular carcinoma with portal vein tumor thrombus. *Int. J. Radiat. Oncol. Biol. Phys.* **73**(3):824–31; 2009.
21. Motosugi, U.; Ichikawa, T.; Araki, T. Rules, roles, and room for discussion in gadoxetic acid-enhanced magnetic resonance liver imaging: current knowledge and future challenges. *Magn. Reson. Med. Sci.* **12**(3):161–75; 2013.
22. Verloh, N.; Haimerl, M.; Zeman, F.; *et al*. Assessing liver function by liver enhancement during the hepatobiliary phase with Gd-EOB-DTPA-enhanced MRI at 3 tesla. *Eur. Radiol.* **24**(5):1013–9; 2014.
23. Sanuki, N.; Takeda, A.; Oku, Y.; *et al*. Threshold doses for focal liver reaction after stereotactic ablative body radiation therapy for small hepatocellular carcinoma depend on liver function: evaluation on magnetic resonance imaging with Gd-EOB-DTPA. *Int. J. Radiat. Oncol. Biol. Phys.* **88**(2):306–11; 2014.
24. Nakamura, Y.; Kimura, T.; Higaki, T.; *et al*. Clinical utility of gadoxetate disodium-enhanced hepatic MRI for stereotactic body radiotherapy of hepatocellular carcinoma. *Jpn. J. Radiol.* **33**(10):627–35; 2015.
25. Nakamura, Y.; Toyota, N.; Shuji, D.; *et al*. Clinical significance of the transitional phase at gadoxetate disodium-enhanced hepatic MRI for the diagnosis of hepatocellular carcinoma: preliminary results. *J. Comput. Assist. Tomogr.* **35**(6):723–7; 2011.

26. Insight Segmentation and Registration Toolkit (ITK), http://itk.org. Accessed May 20, 2015.
27. Motosugi, U.; Ichikawa, T.; Sou, H.; *et al*. Liver parenchymal enhancement of hepatocyte-phase images in Gd-EOB-DTPA-enhanced MR imaging: which biological markers of the liver function affect the enhancement? *J. Magn. Reson. Imaging* **30**(5):1042–6; 2009.
28. de Graaf, W.; Bennink, R.J.; Vetelainen, R.; *et al*. Nuclear imaging techniques for the assessment of hepatic function in liver surgery and transplantation. *J. Nucl. Med.* **51**(5):742–52; 2010.
29. Thian, Y.L.; Riddell, A.M.; Koh, D.M. Liver-specific agents for contrast-enhanced MRI: role in oncological imaging. *Cancer Imaging* **13**(4):567–79; 2013.
30. Nilsson, H.; Blomqvist, L.; Douglas, L.; *et al*. Gd-EOB-DTPA-enhanced MRI for the assessment of liver function and volume in liver cirrhosis. *Br. J. Radiol.* **86**(1026):20120653; 2013.
31. Asayama, Y.; Tajima, T.; Nishie, A.; *et al*. Uptake of Gd-EOB-DTPA by hepatocellular carcinoma: radiologic-pathologic correlation with special reference to bile production. *Eur. J. Radiol.* **80**(3):e243–8; 2011.
32. Tamada, T.; Ito, K.; Sone, T.; *et al*. Gd-EOB-DTPA enhanced MR imaging: evaluation of biliary and renal excretion in normal and cirrhotic livers. *Eur. J. Radiol.* **80**(3):e207–11; 2011.
33. Van Beers, B.E.; Pastor, C.M.; Hussain, H.K. Primovist, Eovist: what to expect? *J. Hepatol.* **57**(2):421–9; 2012.
34. Geisel, D.; Ludemann, L.; Froling, V.; *et al*. Imaging-based evaluation of liver function: comparison of 99mTc-mebrofenin hepatobiliary scintigraphy and Gd-EOB-DTPA-enhanced MRI. *Eur. Radiol.* **25**(5):1384–91; 2015.
35. Motosugi, U.; Ichikawa, T.; Oguri, M.; *et al*. Staging liver fibrosis by using liver-enhancement ratio of gadoxetic acid-enhanced MR imaging: comparison with aspartate aminotransferase-to-platelet ratio index. *Magn. Reson. Imaging* **29**(8):1047–52; 2011.
36. Watanabe, H.; Kanematsu, M.; Goshima, S.; *et al*. Staging hepatic fibrosis: comparison of gadoxetate disodium enhanced and diffusion weighted MR imaging. Preliminary observations. *Radiology* **259**:142–50; 2011.
37. Motosugi, U.; Ichikawa, T.; Tominaga, L.; *et al*. Delay before the hepatocyte phase of Gd-EOB-DTPA-enhanced MR imaging: is it possible to shorten the examination time? *Eur. Radiol.* **19**(11):2623–9; 2009.
38. Radiation Therapy Oncology Group 1112, *Randomized phase III study of Sorafenib versus Stereotactic Body Radiation Therapy followed by Sorefenib in Hepatocellular Carcinoma*. Version Date February 23, 2016. 2016. Available at: https://www.rtog.org/ClinicalTrials/ProtocolTable/StudyDetails.aspx?action=openFile&FileID=13150. Accessed September 23, 2017.
39. Lavrenkov, K.; Singh, S.; Christian, J.A.; *et al*. Effective avoidance of a functional SPECT-perfused lung using intensity modulated radiotherapy (IMRT) for non-small cell lung cancer (NSCLC): an update of a planning study. *Radiother. Oncol.* **91**(3):349–52; 2009.